Supporting Information:
Contributions of individual reactive biogenic volatile organic compounds to organic nitrates above a mixed forest

K. A. Pratt[1], L. H. Mielke[1*], P. B. Shepson[1,2,3], A. M. Bryan[4], A. L. Steiner[4], J. Ortega[5†], R. Daly[5‡], D. Helmig[5], C. S. Vogel[6], S. Griffith[7], S. Dusanter[7-9], P. S. Stevens[7,10], M. Alaghmand[1]

[1]Department of Chemistry, Purdue University, West Lafayette, IN USA
[2]Department of Earth and Atmospheric Sciences, Purdue University, West Lafayette, IN USA
[3]Purdue Climate Change Research Center, Purdue University, West Lafayette, IN USA
[4]Department of Atmospheric, Oceanic and Space Sciences, University of Michigan, Ann Arbor, MI USA
[5]Institute of Arctic and Alpine Research, University of Colorado, Boulder, CO USA
[6]University of Michigan Biological Station, Pellston, MI USA
[7]School of Public and Environmental Affairs, Indiana University, Bloomington, IN USA
[8]Université Lille Nord de France, Lille, France
[9]École des Mines de Douai, Douai, France
[10]Department of Chemistry, Indiana University, Bloomington, IN USA

[*]Now at: School of Public and Environmental Affairs, Indiana University, Bloomington, IN USA
[†]Now at: Atmospheric Chemistry Division, Earth System Laboratory, National Center for Atmospheric Research, Boulder, CO USA
[‡]Now at: Air Pollution Prevention and Control Division, National Risk Management Research Laboratory, U.S. Environmental Protection Agency, Research Triangle Park, NC USA

Correspondence to: K.A. Pratt (kapratt@purdue.edu)

2.2 One-dimensional model description

Future forest composition

Stem density of aspen trees at UMBS and relative proportions of hardwood and pine species and size were estimated in a 1.4 km^2 area of the UMBS forest in 2010 by measuring tree diameter at breast height (DBH, 1.37 m) of all trees with a DBH $\geq$ 8.0 cm in 101 – 800 m^2 plots. For this exercise, all aspen trees were assumed to be replaced by either northern hardwood or upland pine assemblages of like DBH and stem density. Dry leaf mass of each of the replacement species was estimated from biomass equations developed in the Great Lake States or northeastern U.S. in the form $M = aD^b$, where M is foliage dry mass, D is DBH, and a and b are species/site specific parameters (Ribe, 1973; Pastor and Bockheim, 1981; Young et al., 1981; Crow and Erdmann, 1983; Hocker and Early, 1983; Perala and Alban, 1994; Ter-Michaelian and Korzukhin, 1997). From the 2010 census at UMBS we found the mean DBH of aspen trees was 25.0 cm at a density of 22300 stems km^{-2} or 32% of the trees in the forest. The proportions of species in the pine and northern hardwood assemblages were determined from the 2010 census and foliage biomass estimated assuming a complete replacement of aspen with either pine or northern hardwood assemblages (Table S2). For scaling emission rates for temperature, average β-factors for the two future forest scenarios were based on the projected forest composition and associated individual BVOC emissions. For the upland pines future forest scenario, monoterpene (MT) and sesquiterpene (SQT) β-factors were calculated to be 0.19 K^{-1} and 0.14 K^{-1}, respectively. For the northern hardwoods future forest scenario, the SQT β-factor was calculated to be 0.15 K^{-1}; due to uncertainties in the measured aspen MT β-factor, the average MT β-factor (0.14 K^{-1}) was used.

BVOC emissions

Normalized fluxes, measured during branch-enclosure sampling, for the three emission scenarios (base, maximum, and minimum) are shown in Table S3. For the base scenario, the emission rates of all BVOCs were scaled to account for measurement uncertainties. For isoprene, emission rates were scaled by -30% for the base production rate scenario, with no scaling for the maximum production rate scenario and scaling by -66% for the minimum production rate scenario. Previously, Pressley et al. (2005) reported an uncertainty in isoprene eddy covariance measurements at UMBS of ±32-66%. However, similar to the modeling study of Ortega et al. (2007), morning (5:30-10:30 EST) isoprene emissions were overestimated; therefore, for all production rate scenarios, isoprene emission rates during this time period were also scaled (by -9% to -83%, with 0.5 h resolution) according to previously documented average overestimations by Ortega et al. (2007); this adjustment is not reflected in Table S3.

For MTs and other BVOCs, the base production rate scenario included scaling emission rates by +107%; for the maximum and minimum production rate scenarios, scaling by +107% and +10%, respectively, was completed. For these species, Ortega et al. (2007; 2008) previously reported a measurement uncertainty of 27%, as well as reported average sampling losses of ~20-30% [range of 10-80%]. For SQTs, the base production rate scenario included scaling emission rates by +130%, with scaling by +130% and +10% for the maximum and minimum production rate scenarios, respectively. This accounts for the previously reported a measurement uncertainty of 50% for SQTs, as well as reported average sampling losses of ~20-30% [range of 10-80%] (Ortega et al., 2007; 2008). In addition, for temperature dependence scaling of the MTs, SQTs, and other BVOCs, upper and lower quartile β-factors were applied for the minimum and maximum production rate scenarios. Also, for the MTs, SQTs, and other BVOCs, the

maximum and minimum production rate scenarios account for tree-to-tree variability during branch enclosure measurements, as well as 95% confidence intervals associated with measurements of mean green-leaf dry mass of the various tree species. Thus, the production rate scenarios account for uncertainty and variability in emission rate measurements.

Calculated NO_3 concentrations

Nitrate radicals are primarily produced by reaction of NO_2 with O_3 and generally removed by photolysis and reaction with NO, as described by reactions 1-3:

$$NO_2 + O_3 \rightarrow NO_3 + O_2 \qquad (R1)$$

$$NO_3 + NO \rightarrow 2NO_2 \qquad (R2)$$

$$NO_3 + h\upsilon \rightarrow NO_2 + O(^3P) \qquad (R3a)$$

$$\rightarrow NO + O_2 \qquad (R3b)$$

The NO_3 production and loss reactions included in the box model are described in Table S4 with their corresponding rate constants. Total sesquiterpene (SQT) concentrations were estimated using the noontime average [SQT]/[MT] ratio measured by Kim et al. (2009) at the PROPHET site (July-August 2005) and the measured total MT concentration for July-August 2008 (PTR-LIT). NO_3 photolysis rates were calculated using the National Center for Atmospheric Research (NCAR) tropospheric ultraviolet and visible (TUV) radiation model (http://cprm.acd.ucar.edu/Models/TUV/) with total column ozone obtained from the Ozone Monitoring Instrument (OMI) on the Aura spacecraft (http://jwocky.gsfc.nasa.gov/teacher/ozone_overhead.html). NO_3 reached steady state within ~0.5-8 min in the box model calculations, which were repeated to create an average 0.5 hr resolution NO_3 diurnal profile for sunny days in July-August 2008.

Table S1. BVOCs identified during branch-enclosure emission measurements for UMBS tree species. Corresponding reaction rate constants (units of cm^3 $molec^{-1}$ s^{-1}) for OH, O_3, and NO_3 at 298 K (k_{OH}, k_{O3}, and k_{NO3}, respectively) and $RONO_2$ yields for reactions with OH and NO_3 (γ_{OH} and γ_{NO3}, respectively) are included for each BVOC identified. Individual BVOCs are displayed in order of simulated $RONO_2$ contribution; BVOCs contributing >0.5 ppt $RONO_2$ (at ~12 m above forest canopy) at any time are shown in Table 1.

BVOC	Structure	k_{OH} k_{O3} k_{NO3} (cm^3 $molec^{-1}$ s^{-1})	$RONO_2$: γ_{OH} γ_{NO3}
β-linalool ($C_{10}H_{18}O$)	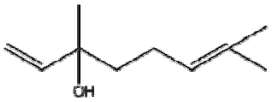	1.59 x 10^{-10} a) 4.3 x 10^{-16} a) 1.12 x 10^{-11} a)	0.30 b) 0.31 c)
camphene ($C_{10}H_{16}$)	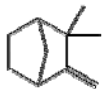	5.30 x 10^{-11} d) 9.0 x 10^{-19} d) 6.6 x 10^{-13} d)	0.23 e) 0.31 c)
α-farnesene ($C_{15}H_{24}$)	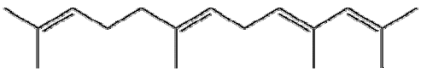	2.19 x 10^{-10} f) 5.94 x 10^{-16} f) 2.1 x 10^{-11} g)	0.29 h) 0.31 c)
β-phellandrene ($C_{10}H_{16}$)	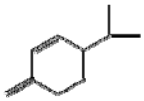	1.68 x 10^{-10} d) 4.7 x 10^{-17} d) 8.0 x 10^{-12} d)	0.18 h) 0.31 c)
α-phellandrene ($C_{10}H_{16}$)	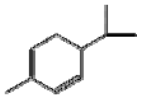	3.13 x 10^{-10} d) 3.0 x 10^{-15} d) 7.3 x 10^{-11} d)	0.18 h) 0.31 c)
terpinolene ($C_{10}H_{16}$)	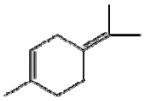	2.25 x 10^{-10} d) 1.9 x 10^{-15} d) 9.7 x 10^{-11} d)	0.18 h) 0.31 c)
allo-ocimene ($C_{10}H_{16}$)		2.36 x 10^{-10} i) 4.16 x 10^{-16} i) 1.1 x 10^{-11} g)	0.18 h) 0.31 c)
dimethylnonatriene ($C_{11}H_{18}$)	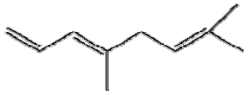	2.32 x 10^{-10} i) 7.50 x 10^{-16} i) 9.6 x 10^{-12} g)	0.20 h) 0.31 c)
α-terpineol ($C_{10}H_{18}O$)	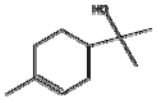	1.9 x 10^{-10} j) 3.0 x 10^{-16} j) 1.60 x 10^{-11} k)	0.30 b) 0.31 c)
α-terpinene ($C_{10}H_{16}$)	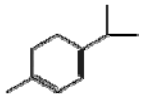	3.63 x 10^{-10} d) 2.1 x 10^{-14} d) 1.4 x 10^{-11} d)	0.18 h) 0.31 c)
β-selinene ($C_{15}H_{24}$)	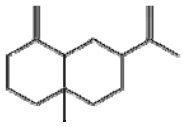	1.17 x 10^{-10} i) 2.40 x 10^{-17} i) 6.5 x 10^{-13} g)	0.29 h) 0.31 c)

β-caryophyllene ($C_{15}H_{24}$)	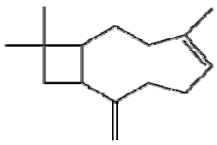	1.97×10^{-11} d) 1.16×10^{-14} d) 1.9×10^{-11} d)	0.29 h) 0.31 c)
δ-cadinene ($C_{15}H_{24}$)	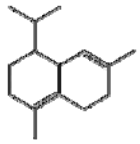	2.11×10^{-10} i) 1.63×10^{-15} i) 5.2×10^{-11} g)	0.29 h) 0.31 c)
β-bourbonene ($C_{15}H_{24}$)	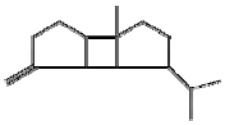	6.19×10^{-11} i) 1.2×10^{-17} i) 3.5×10^{-13} g)	0.29 h) 0.31 c)
α-copaene ($C_{15}H_{24}$)	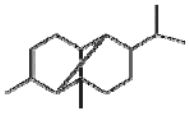	9.00×10^{-11} d) 1.60×10^{-16} d) 1.60×10^{-11} d)	0.29 h) 0.31 c)
4-carene ($C_{10}H_{16}$)	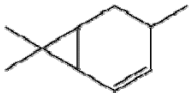	5.81×10^{-11} i) 2.00×10^{-16} i) 8.9×10^{-13} g)	0.18 e) 0.31 f)
4-terpineol ($C_{10}H_{18}O$)	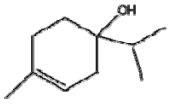	1.04×10^{-10} i) (<)1×10^{-20} i) 1.4×10^{-16} g)	0.30 b) 0.31 c)
α-selinene ($C_{15}H_{24}$)	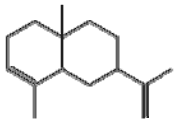	1.51×10^{-10} i) 4.42×10^{-16} i) 5.8×10^{-12} g)	0.29 h) 0.31 c)
camphor ($C_{10}H_{16}O$)	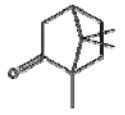	4.30×10^{-12} d) (<)7×10^{-20} l) (<)3.00×10^{-16} d)	0.31 m) 0.31 c)
3-carene ($C_{10}H_{16}$)	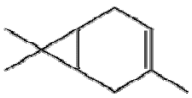	8.80×10^{-11} d) 3.7×10^{-17} d) 9.1×10^{-12} d)	0.18 h) 0.31 c)
β-elemene ($C_{15}H_{24}$)	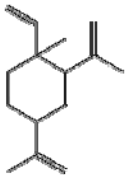	1.40×10^{-10} i) 2.6×10^{-17} i) 6.3×10^{-11} g)	0.29 h) 0.31 c)
α-cubebene ($C_{15}H_{24}$)	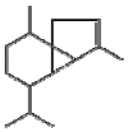	1.00×10^{-10} i) 4.30×10^{-16} d) 7.9×10^{-12} g)	0.29 h) 0.31 c)
1,8-cineole ($C_{10}H_{18}O$)	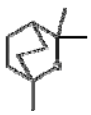	1.11×10^{-11} n) (<)1.5×10^{-19} o) 1.7×10^{-16} n)	0.52 p) 0.31 c)

D germacrene ($C_{15}H_{24}$)	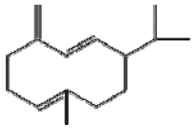	2.40×10^{-10} i) 6.10×10^{-16} i) 6.4×10^{-12} g)	0.29 h) 0.31 c)
o-cymene ($C_{10}H_{14}$)	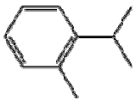	8.54×10^{-12} i) (<)5×10^{-20} q) 9.9×10^{-16} q)	0.03 r) 0.31 c)
allo- aromadendrene ($C_{15}H_{24}$)	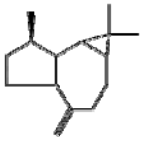	6.25×10^{-11} i) 1.20×10^{-17} i) 3.5×10^{-13} g)	0.29 h) 0.31 c)
γ-muurolene ($C_{15}H_{24}$)	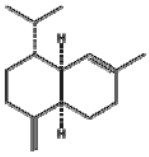	1.56×10^{-10} i) 4.42×10^{-16} i) 5.9×10^{-12} g)	0.29 h) 0.31 c)
β-cubebene ($C_{15}H_{24}$)	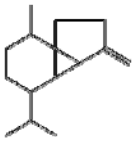	6.54×10^{-11} i) 1.20×10^{-17} i) 3.5×10^{-13} g)	0.29 h) 0.31 c)
α-muurolene ($C_{15}H_{24}$)	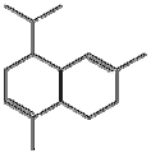	1.90×10^{-10} i) 8.6×10^{-16} i) 1.1×10^{-11} g)	0.29 h) 0.31 c)
β-gurjunene ($C_{15}H_{24}$)	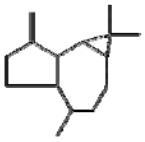	6.01×10^{-11} i) 1.20×10^{-17} i) 3.5×10^{-13} g)	0.29 h) 0.31 c)
borneol ($C_{10}H_{18}O$)	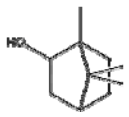	1.14×10^{-11} i) (<)1×10^{-20} d) 4.6×10^{-15} s)	0.52 p) 0.31 c)
β-farnesene ($C_{15}H_{24}$)	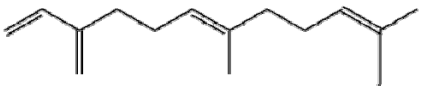	2.88×10^{-10} f) 6.86×10^{-16} f) 9.3×10^{-12} g)	0.29 h) 0.31 c)
α-humulene ($C_{15}H_{24}$)	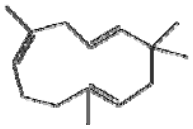	2.93×10^{-10} d) 1.17×10^{-14} d) 3.90×10^{-11} d)	0.29 h) 0.31 c)
cis- and *trans*- linalool oxide ($C_{10}H_{18}O_2$)	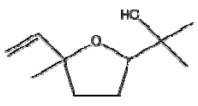	6.68×10^{-11} i) 1.75×10^{-18} i) 4.6×10^{-14} g)	0.30 b) 0.31 c)
β-bisabolene ($C_{15}H_{24}$)	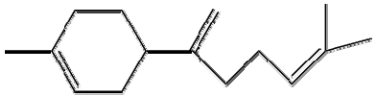	2.4×10^{-11} i) 8.7×10^{-16} i) 9.2×10^{-12} g)	0.29 h) 0.31 c)

p-cymene ($C_{10}H_{14}$)	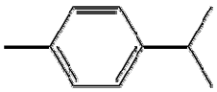	1.51 x 10^{-11} h) (<)5 x 10^{-20} o) 9.9 x 10^{-16} n)	0.03 r) 0.31 c)
germacrene B ($C_{15}H_{24}$)	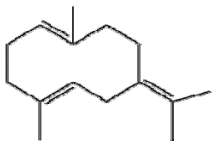	2.90 x 10^{-10} i) 2.06 x 10^{-15} i) 4.3 x 10^{-11} g)	0.29 h) 0.31 c)
aromadendrene ($C_{15}H_{24}$)	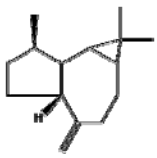	1.50 x 10^{-10} t) 6.50 x 10^{-15} u) 3.5 x 10^{-13} g)	0.29 h) 0.31 c)
α-cedrene ($C_{15}H_{24}$)		6.70 x 10^{-11} d) 2.80 x 10^{-17} d) 8.20 x 10^{-12} d)	0.29 h) 0.31 c)
tricyclene ($C_{10}H_{16}$)		2.66 x 10^{-12} i) (<)1 x 10^{-23} d) 1.1 x 10^{-15} s)	0.31 m) 0.31 c)
α-*trans*-bergamotene ($C_{15}H_{24}$)	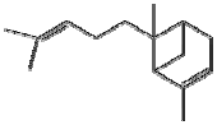	1.80 x 10^{-10} i) 8.60 x 10^{-16} i) 9.6 x 10^{-12} g)	0.29 h) 0.31 c)
camphene hydrate ($C_{10}H_{18}O$)	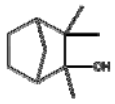	9.43 x 10^{-12} i) (<)1 x 10^{-20} d) 6.4 x 10^{-16} s)	0.52 p) 0.31 c)
γ-cadinene ($C_{15}H_{24}$)	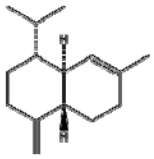	1.56 x 10^{-10} i) 3.20 x 10^{-14} t) 5.9 x 10^{-12} g)	0.29 h) 0.31 c)
para-cymenene ($C_{10}H_{16}$)	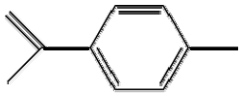	5.7 x 10^{-11} i) 1.4 x 10^{-16} i) 1.5 x 10^{-12} v)	0.18 h) 0.31 c)
norbornene (C_7H_{10})		1.0 x 10^{-10} d) 1.27 x 10^{-17} d) 7.0 x 10^{-13} d)	0.11 h) 0.31 c)
cyclofenchone ($C_{10}H_{16}$)	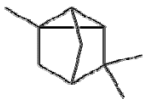	3.54 x 10^{-12} i) (<)1 x 10^{-23} d) 1.4 x 10^{-15} s)	0.31 m) 0.31 c)

a) Atkinson et al. (1995)

b) Estimated based on Arey et al. (2001), Espada and Shepson (2005), and O'Brien et al. (1998)

c) Average of α-pinene, β-pinene, and limonene yields

d) Atkinson and Arey (2003)
e) β-pinene used as a proxy
f) Kim et al. (2011)
g) Estimated based on Pfrang et al. (2006)
h) Estimated based on Arey et al. (2001) and O'Brien et al. (1998)
i) Estimated using the Environmental Protection Agency's Estimation Program Interface Suite (USEPA, 2010)
j) Wells (2005)
k) Jones and Ham (2008)
l) Reissell et al. (2001)
m) Estimated based on Arey et al. (2001)
n) Corchnoy and Atkinson (1990)
o) Atkinson et al. (1990)
p) Estimated based on Arey et al. (2001) and Espada and Shepson (2005)
q) *p*-cymene used as a proxy
r) *p*-xylene (Espada et al., 2005) used as a proxy
s) Estimated based on Kerdouci et al. (2010)
t) Ng et al. (2007)
u) Pollmann et al. (2005)
v) styrene (Atkinson and Arey, 2003) used as a proxy

Table S2. Estimated leaf dry mass and species proportions for replacement of aspen in the future UMBS forest. Values in parentheses are ± standard error.

Assemblage/species	Leaf dry mass ($g \cdot m^{-2}$)	Species proportions (%)
Northern Hardwoods		
Acer rubrum	102.8 (19.5)	70.5
Acer saccharum	28.3 (1.6)	15.5
Fagus grandifolia	26.1 (1.7)	14.0
Upland Pines		
Pinus strobus	233.4 (35.0)	89.0
Pinus resinosa	44.1 (4.4)	11.0

Table S3. Normalized fluxes (μg C m^{-2} h^{-1}) for three emission scenarios (base, maximum, and minimum production). Fluxes were normalized to a standard photosynthetic active radiation flux of 1000 μmol m^{-2} s^{-1} and a standard temperature of 303.15 K.

BVOC Class	Base	Maximum	Minimum
Isoprene	8141	14375	3909
Monoterpenes	667	1357	148
Sesquiterpenes	94	274	7
Other BVOCs	61	119	14

Table S4. NO_3 production and loss reactions included in the box model with corresponding rate constants.

Reaction	k (cm^3 $molec^{-1}$ s^{-1})	Reference
$NO_3 + NO \rightarrow 2NO_2$	2.6×10^{-11}	(Atkinson et al., 2004)
$NO_3 + NO_2 \rightarrow N_2O_5$	1.9×10^{-12}	(Atkinson et al., 2004)
$NO_3 + OH \rightarrow NO_2 + HO_2$	2.0×10^{-11}	(Atkinson et al., 2004)
$NO_3 + HO_2 \rightarrow HNO_3 + O_2$	4.0×10^{-12}	(Atkinson et al., 2004)
$NO_3 + RO_2 \rightarrow RO + NO_2$	4.0×10^{-12}	Assumed same as HO_2 reaction
NO_3 + Isoprene → Products	7.0×10^{-13}	(Atkinson and Arey, 2003)
NO_3 + MTs → Products	1.4×10^{-11}	Emission weighted average (see Table 1 for individual k_{NO3})
NO_3 + SQTs → Products	1.7×10^{-11}	Emission weighted average (see Table 1 for individual k_{NO3})
NO_3 + MACR → Products	3.4×10^{-15}	(Atkinson and Arey, 2003)
NO_3 + MVK → Products	(<)6×10^{-15}	(Atkinson and Arey, 2003)
$NO_2 + O_3 \rightarrow NO_3 + O_2$	3.5×10^{-17}	(Atkinson et al., 2004)
$NO + O_3 \rightarrow NO_2 + O_2$	1.8×10^{-14}	(Atkinson et al., 2004)
$N_2O_5 \rightarrow NO_3 + NO_2$	6.9×10^{-2} s^{-1}	(Atkinson et al., 2004)
NO_3 → particles	4.0×10^{-3} s^{-1}	(Hurst et al., 2001)
N_2O_5 → particles	9.3×10^{-4} s^{-1}	(Hurst et al., 2001)
$NO_3 + hv \rightarrow NO_2 + O$	variable	NCAR TUV model
$NO_3 + hv \rightarrow NO + O_2$	variable	NCAR TUV model

Table S5. First generation isoprene oxidation products with yields from isoprene oxidation, oxidation rate constants (units of cm^3 $molec^{-1}$ s^{-1}), and $RONO_2$ yields. Methacrolein (MACR) and methyl vinyl ketone (MVK) yields by OH oxidation are defined within the model based on the availability of NO, as represented by β (defined in the text as the fraction of time RO_2 reacts with NO versus HO_2 and RO_2), using high and low NO_x chamber yields from Ruppert and Becker (2000). The structures of $RONO_2$ products from the oxidation of these first generation isoprene oxidation products were estimated, and corresponding rate constants were estimated (Atkinson and Arey, 2003; Kerdouci et al., 2010; USEPA, 2010) to predict the removal of the nitrates.

First Generation Isoprene Oxidation Product	Structure	Isoprene γ_{OH} γ_{O3} γ_{NO3}	k_{OH} k_{O3} k_{NO3}	$RONO_2$: γ_{OH} γ_{NO3}
MACR	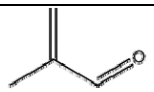	0.18-0.20 a) 0.39 b) 0.035 b)	2.9×10^{-11} c) 1.2×10^{-18} c) 3.4×10^{-15} c)	0.0705 d) 0.24 e)
MVK	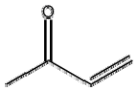	0.15-0.31 a) 0.16 b) 0.035 b)	2.0×10^{-11} c) 5.2×10^{-18} c) (<)6.0×10^{-16} c)	0.11 d) 0.24 e)
IP-HMY	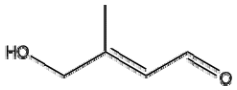	0.15 e) 0 e) 0 e)	7.0×10^{-11} f) 1.0×10^{-17} f) 1.0×10^{-13} f)	0.075 e) 0.20 e)
IP-MHY	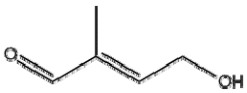	0.13 e) 0 e) 0.32 f)	7.0×10^{-11} f) 1.0×10^{-17} f) 1.0×10^{-13} f)	0.075 e) 0.20 e)

a) (Ruppert and Becker, 2000)
b) (Atkinson and Arey, 1998)
c) (Atkinson et al., 2006)
d) (Paulot et al., 2009)
e) Estimation by Costa (2011)
f) (Carter and Atkinson, 1996)

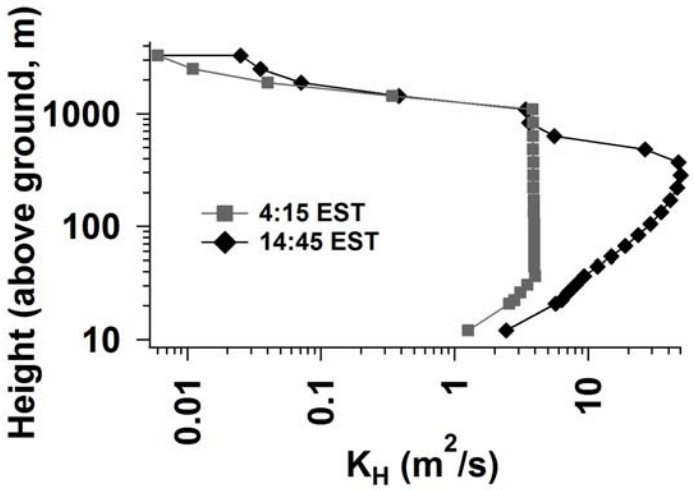

Figure S1. Modeled thermal eddy diffusivity (K_H) profiles for UMBS in the summer at 4:15 and 14:45 EST.

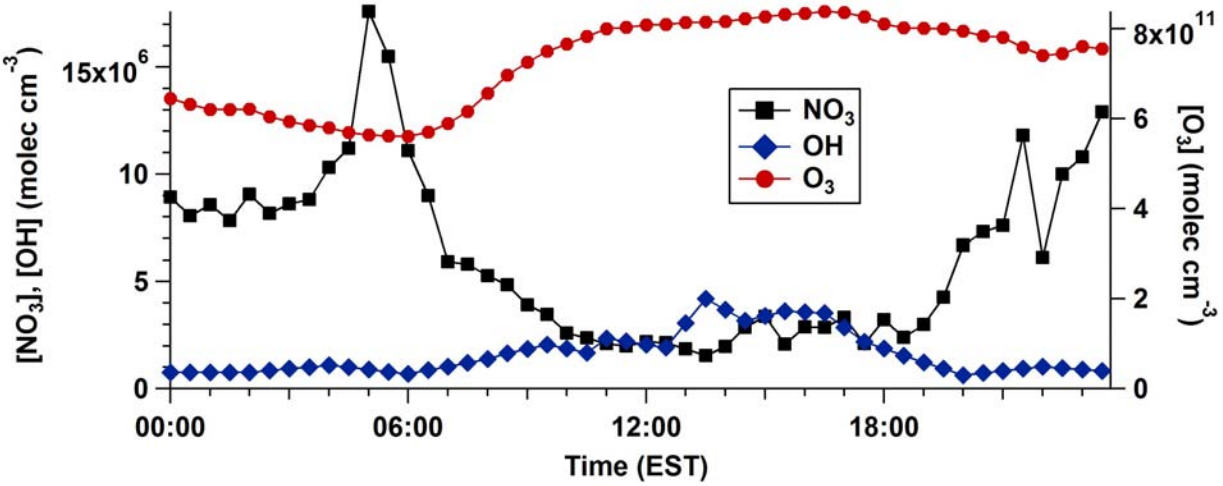

Figure S2. Diurnal cycles of the average concentrations of NO_3 (modeled), OH (measured), and O_3 (measured), used in the model, for 32 m above ground (10 m above canopy).

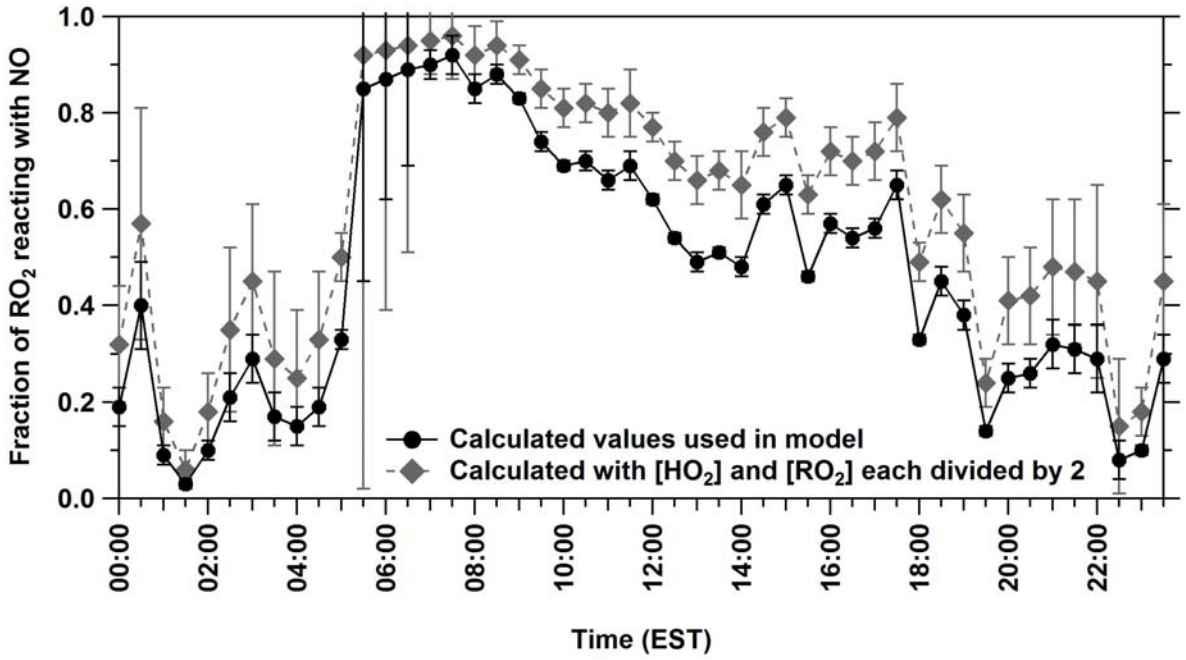

Figure S3. Calculated average diurnal cycle of δ, used in the model and defined in Section 2.2.4 as the fraction of time RO_2 reacts with NO versus HO_2 and RO_2. If we assume that the actual "HO_2" concentrations were half the measured values due to an interference from isoprene RO_2, this translates to an average diurnal increase in δ of 0.12 (range of 0.02-0.17); as shown here, the primary effect would be a relative increase in $RONO_2$ production in the mid-day and nighttime.

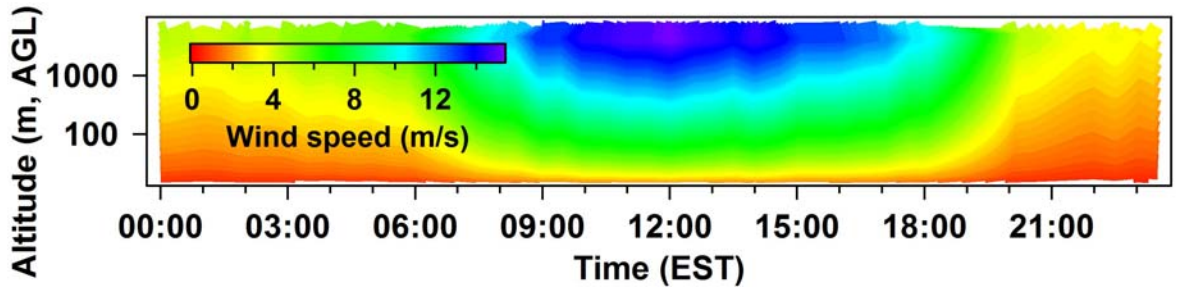

Figure S4. Diurnal cycle of calculated wind speed (0.5 hour time resolution) versus altitude. The logarithmic wind profile scaling (equation *XII*) does not account for atmospheric stability and may underestimate nighttime winds, particularly above 100 m.

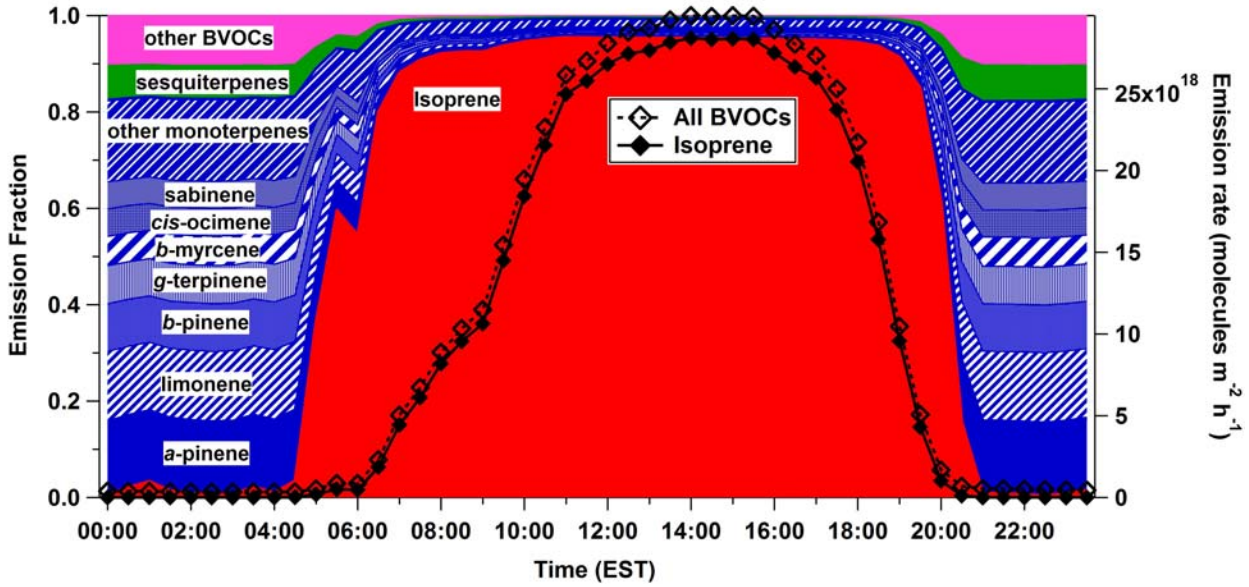

Figure S5. Diurnal cycle of calculated absolute (lines, right axis) and fractional (colors, left axis) emission rates (base scenario) of BVOCs at UMBS.

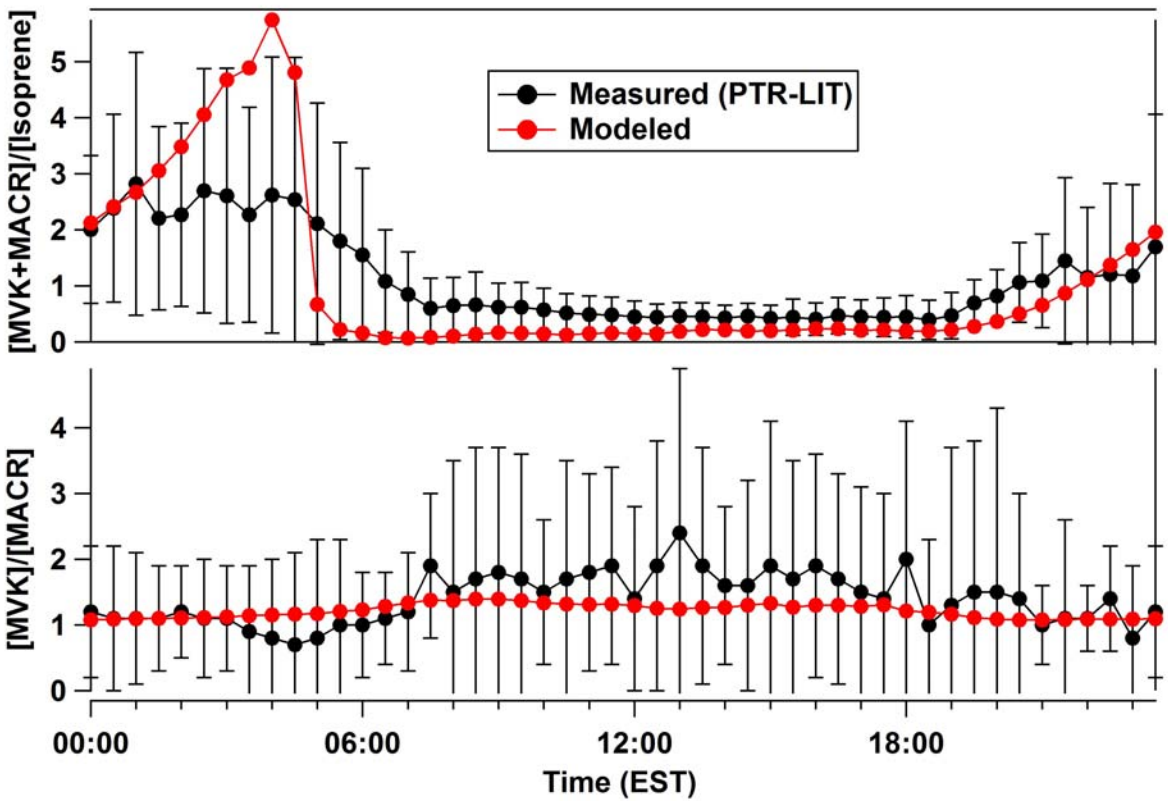

Figure S6. Diurnal cycles of modeled and measured [methyl vinyl ketone (MVK) + methacrolein (MACR)]/[isoprene] and [MVK]/[MACR)] at ~12 m above the forest canopy. July-August 2008 measurements were completed using a proton-transfer reaction linear ion trap mass spectrometer (PTR-LIT) (Mielke et al., 2010). For nighttime periods when few PTR-LIT MS/MS measurements of [MVK] and [MACR] were made, PTR-LIT [MVK+MACR] data were utilized to obtain estimated [MVK] and [MACR] by applying 0.5 h average [MVK]/[MACR] from the previous UMBS study by Apel et al. (2002). Sensitivity to uncertainties and variability are indicated by error bars.

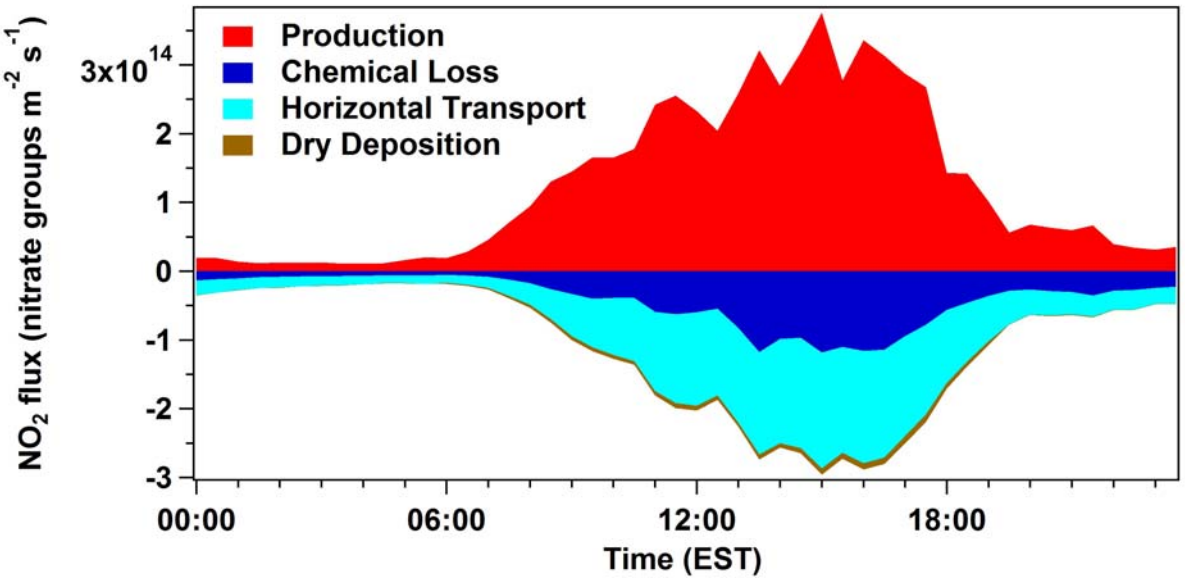

Figure S7. Modeled diurnal cycle of total column nitrate flux due to addition (organic nitrate production) and loss processes (chemical reaction, horizontal advection, and dry deposition). Loss of individual primary and secondary nitrates are shown, as well as the production of secondary nitrates, with dinitrate fluxes multiplied by two to represent the two nitrate groups present within these molecules.

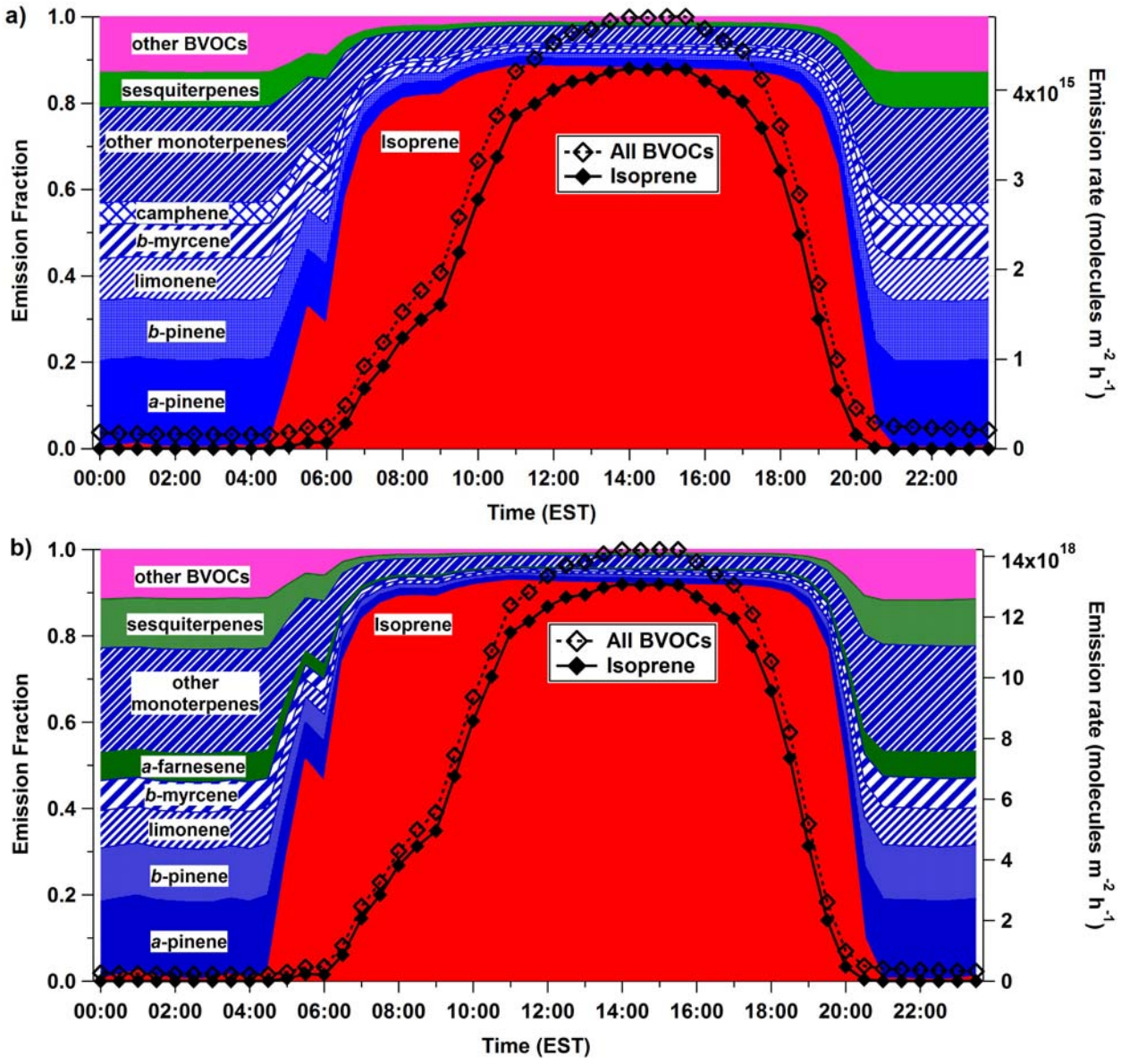

Figure S8. Diurnal cycles of calculated absolute (lines, right axis) and fractional (colors, left axis) emission rates (base scenario) of BVOCs at UMBS following replacement of aspen by a) northern hardwoods or b) upland pine.

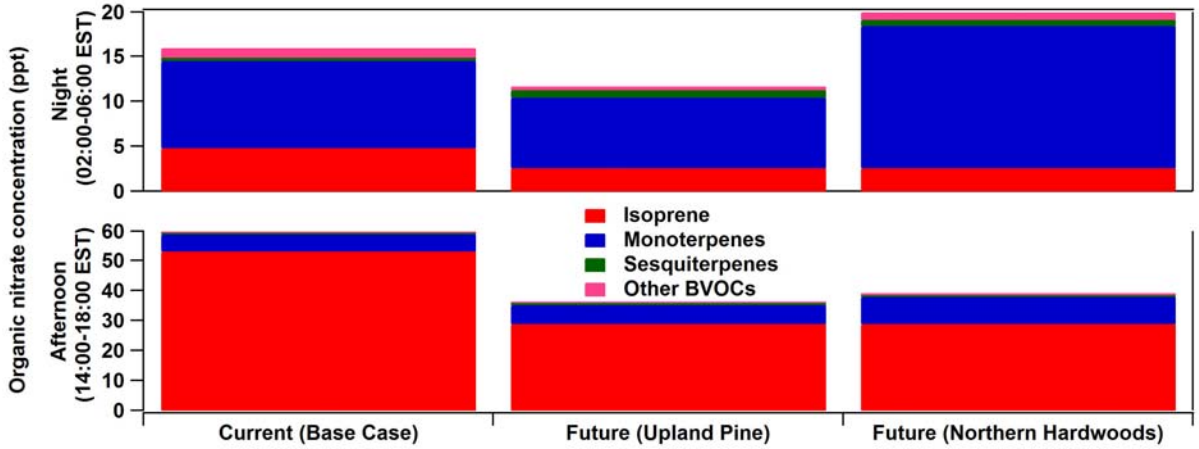

Figure S9. Comparison of simulated biogenic organic nitrate concentrations at ~12 m above the forest canopy for the current forest (base case), compared to the two future forest scenarios (upland pine and northern hardwoods).

References

Apel, E. C., Riemer, D. D., Hills, A., Baugh, W., Orlando, J., Faloona, I., Tan, D., Brune, W., Lamb, B., Westberg, H., Carroll, M. A., Thornberry, T., and Geron, C. D.: Measurement and interpretation of isoprene fluxes and isoprene, methacrolein, and methyl vinyl ketone mixing ratios at the PROPHET site during the 1998 Intensive, J. Geophys. Res., 107, doi:10.1029/2000JD000225, 2002.

Arey, J., Aschmann, S. M., Kwok, E. S. C., and Atkinson, R.: Alkyl nitrate, hydroxy nitrate, and hydroxycarbonyl formation from the NO_x-air photooxidations of C_5-C_8 *n*-alkanes, J. Phys. Chem. A, 105, 1020-1027, 2001.

Atkinson, R., Hasegawa, J., and Aschmann, S. M.: Rate constants for the gas-phase reactions of O_3 with a series of monoterpenes and related compounds at 296 ± 2 K, Int. J. Chem. Kinet., 22, 871-887, 1990.

Atkinson, R., Arey, J., Aschmann, S. M., Corchnoy, S. B., and Shu, Y.: Rate constants for the gas-phase reactions of *cis*-3-hexen-1-ol, *cis*-3-hexenylacetate, *trans*-2-hexenal, and linalool with OH and NO_3 radicals and O_3 at 296 ± 2 K, and OH radical formation yields from the O_3 reactions, Int. J. Chem. Kinet., 27, 941-955, 1995.

Atkinson, R., and Arey, J.: Atmospheric chemistry of biogenic organic compounds, Acc. Chem. Res., 31, 574-583, 1998.

Atkinson, R., and Arey, J.: Atmospheric degradation of volatile organic compounds, Chem. Rev., 103, 4605-4638, 2003.

Atkinson, R., Baulch, D. L., Cox, R. A., Crowley, J. N., Hampson, R. F., Hynes, R. G., Jenkin, M. E., Rossi, M. J., and Troe, J.: Evaluated kinetic and photochemical data for atmospheric chemistry: Volume I - gas phase reactions of O_x, HO_x, NO_x and SO_x species, Atmos. Chem. Phys., 4, 1461-1738, 2004.

233 Atkinson, R., Baulch, D. L., Cox, R. A., Crowley, J. N., Hampson, R. F., Hynes, R. G., Jenkin,
234 M. E., Rossi, M. J., and Troe, J.: Evaluated kinetic and photochemical data for
235 atmospheric chemistry: Volume II - gas phase reactions of organic species, Atmos.
236 Chem. Phys., 6, 2006.
237 Carter, W. P. L., and Atkinson, R.: Development and evaluation of a detailed mechanism for the
238 atmospheric reactions of isoprene and NO_x, Int. J. Chem. Kinet., 28, 497-530, 1996.
239 Corchnoy, S. B., and Atkinson, R.: Kinetics of the gas-phase reactions of OH and NO_3 radicals
240 with 2-carene, 1,8-cineole, *p*-cymene, and terpinolene, Environ. Sci. Technol., 24, 1497-
241 1502, 1990.
242 Costa, A. W.: Coupling between the carbon and nitrogen cycles in a forested environment,
243 Ph.D., Chemistry, Purdue University, West Lafayette, IN, 279 pp., 2011.
244 Crow, T. R., and Erdmann, G. G.: Weight and volume equations and tables for red maples in the
245 Lake States, U.S. Forest Service Research Paper, NC-242, 14, 1983.
246 Espada, C., Grossenbacher, J. W., Ford, K., Couch, T., and Shepson, P. B.: The production of
247 organic nitrates from various anthropogenic volatile organic compounds, Int. J. Chem.
248 Kinet., 37, 675-685, 2005.
249 Espada, C., and Shepson, P. B.: The production of organic nitrates from atmospheric oxidation of
250 ethers and glycol ethers, Int. J. Chem. Kinet., 37, 686-699, 2005.
251 Hocker, H. W., and Early, D. J.: Biomass and leaf area equations for northern forest species,
252 New Hampshire Agricultural Experiment Station University of New Hampshire Research
253 Report, 102, 27, 1983.
254 Hurst, J. M., Barket, D. J., Herrera-Gomez, O., Couch, T. L., Shepson, P. B., Faloona, I., Tan,
255 D., Brune, W., Westberg, H., Lamb, B., Biesenthal, T., Young, V., Goldstein, A.,

256 Munger, J. W., Thornberry, T., and Carroll, M. A.: Investigation of the nighttime decay
257 of isoprene, J. Geophys. Res., 106, 24335-24346, 2001.
258 Jones, B. T., and Ham, J. E.: α-Terpineol reactions with the nitrate radical: Rate constant and
259 gas-phase products, Atmos. Environ., 42, 6689-6698, 2008.
260 Kerdouci, J., Picquet-Varrault, B., and Doussin, J. F.: Prediction of rate constants for gas-phase
261 reactions of nitrate radical with organic compounds: A new structure-activity
262 relationship, Chem. Phys. Chem., 11, 3909-3920, 2010.
263 Kim, D., Stevens, P. S., and Hites, R. A.: Rate constants for the gas-phase reactions of OH and
264 O3 with β-ocimene, β-myrcene, and α- and β-farnesene as a function of temperature, J.
265 Phys. Chem. A, 115, 500-506, 2011.
266 Kim, S., Karl, T., Helmig, D., Daly, R., Rasmussen, R., and Guenther, A.: Measurement of
267 atmospheric sesquiterpenes by proton transfer reaction-mass spectrometry (PTR-MS),
268 Atmos. Meas. Tech., 2, 99-102, 2009.
269 Mielke, L. H., Pratt, K. A., Shepson, P. B., McLuckey, S. A., Wisthaler, A., and Hansel, A.:
270 Quantitative determination of biogenic volatile organic compounds in the atmosphere
271 using proton-transfer reaction linear ion trap mass spectrometry, Anal. Chem., 82, 7952-
272 7957, 2010.
273 Ng, N. L., Chhabra, P. S., Chan, A. W. H., Surratt, J. D., Kroll, J. H., Kwan, A. J., McCabe, D.
274 C., Wennberg, P. O., Sorooshian, A., Murphy, S. M., Dalleska, N. F., Flagan, R. C., and
275 Seinfeld, J. H.: Effect of NO_x level on secondary organic aerosol (SOA) formation from
276 the photooxidation of terpenes, Atmos. Chem. Phys., 7, 5159-5174, 2007.

277 O'Brien, J. M., Czuba, E., Hastie, D., Francisco, J. S., and Shepson, P. B.: Determination of the
278 hydroxy nitrate yields from the reaction of C_2-C_6 alkenes with OH in the presence of NO,
279 J. Phys. Chem. A, 102, 8903-8908, 1998.
280 Ortega, J., Helmig, D., Guenther, A., Harley, P., Pressley, S., and Vogel, C.: Flux estimates and
281 OH reaction potential of reactive biogenic volatile organic compounds (BVOCs) from a
282 mixed northern hardwood forest, Atmos. Environ., 41, 5479-5495, 2007.
283 Ortega, J., Helmig, D., Daly, R. W., Tanner, D. M., Guenther, A. B., and Herrick, J. D.:
284 Approaches for quantifying reactive and low-volatility biogenic organic compound
285 emissions by vegetation enclosure techniques - Part B: Applications, Chemosphere, 72,
286 365-380, 2008.
287 Pastor, J., and Bockheim, J. G.: Biomass and production of an aspen-mixed hardwood-spodosol
288 ecosystem in northern Wisconsin, Can. J. For. Res., 11, 132-138, 1981.
289 Paulot, F., Crounse, J. D., Kjaergaard, H. G., Kroll, J. H., Seinfeld, J. H., and Wennberg, P. O.:
290 Isoprene photooxidation: new insights into the production of acids and organic nitrates,
291 Atmos. Chem. Phys., 9, 1479-1501, 2009.
292 Perala, D. A., and Alban, D. H.: Allometric biomass estimators for aspen-dominated ecosystems
293 in the Upper Great Lakes, U.S. Forest Service Research Paper, NC-134, 38, 1994.
294 Pfrang, C., King, M. D., Canosa-Mas, C. E., and Wayne, R. P.: Structure-activity relations
295 (SARs) for gas-phase reactions of NO_3, OH and O_3 with alkenes: An update, Atmos.
296 Environ., 40, 1180-1186, 2006.
297 Pollmann, J., Ortega, J., and Helmig, D.: Analysis of atmospheric sesquiterpenes: Sampling
298 losses and mitigation of ozone interferences, Environ. Sci. Technol., 39, 9620-9629,
299 2005.

Pressley, S., Lamb, B., Westberg, H., Flaherty, J., Chen, J., and Vogel, C.: Long-term isoprene flux measurements above a northern hardwood forest, J. Geophys. Res., 110, doi:10.1029/2004JD005523, 2005.

Reissell, A., Arey, J., and Atkinson, R.: Atmospheric chemistry of camphor, Int. J. Chem. Kinet., 33, 56-63, 2001.

Ribe, J. H.: Puckerbrush weight tables, Miscellaneous Report 152, Life Sciences and Agricultural Experiment Station. University of Maine. Orono, ME, 92 pp., 1973.

Ruppert, L., and Becker, K. H.: A product study of the OH radical-initiated oxidation of isoprene: formation of C5-unsaturated diols, Atmos. Environ., 34, 1529-1542, 2000.

Ter-Michaelian, M. T., and Korzukhin, M. D.: Biomass equations for sixty-five North American tree species, Forest Ecol. Manage., 97, 1-24, 1997.

USEPA: Estimation Programs Interface Suite™ for Microsoft® Windows, v 4.0, United State Environmental Protection Agency, Washington, DC, USA, 2010.

Wells, J. R.: Gas-phase chemistry of α-terpineol with ozone and OH radical: Rate constants and products, Environ. Sci. Technol., 39, 6937-6943, 2005.

Young, H. E., Ribe, J. H., and Wainwright, K.: Weight tables for tree and shrub species in Maine, Miscellaneous Report 230, Life Sciences and Agriculture Experiment Station. University of Maine. Orono, ME, 84 pp., 1981.